

Nuclear Science and Technology

Journal homepage: <http://jnst.vn/index.php/nst>



Simulation of gamma reference field at Institute for Nuclear Science and Technology using Monte Carlo method

Bui Duc Ky*, Nguyen Ngoc Quynh, Nguyen Huu Quyet, Dang Thi My Linh, Duong Thi Nhung,
Nguyen Dang Nguyen, Dang Thi Minh Hue

Institute for Nuclear Science and Technology

179 Hoang Quoc Viet Street, Nghia Do Ward, Cau Giay Dist., Hanoi, Vietnam

**Email: duckyb2@gmail.com*

Abstract: This paper presents the characterization of two gamma reference fields of ^{137}Cs and ^{60}Co sources at the Institute for Nuclear Science and Technology. The characterization of the fields in terms of gamma fluence Φ , mean energy, E_ϕ , kerma weighted mean energies, E_K , air kerma, K_{air} , were determined at various distances from the source center by Monte Carlo simulation using MCNP6. The air kerma results were compared with the measurements obtained by using a calibrated ionization chamber. The discrepancy between the simulated and measured air kerma was less than 4.5%. The scattered component was also simulated and calculated. The results of both methods showed that the contribution of the scattered components to the gamma reference field is less than 3%. This contribution comply with the international standard criteria of ISO 4037 (<5%). The results confirmed that the characterization of the gamma reference field could be determined using the simulation code.

Keywords: *Gamma reference field, MCNP6.*

I. INTRODUCTION

The gamma calibration facility was established in the 1990s at the Institute for Nuclear Science and Technology (INST), Vietnam Atomic Energy Institute, and is the first calibration facility for radiation metrology in Vietnam. At that time, the gamma reference field was established using a ^{137}Cs radiation source for calibrating ionizing radiation instruments. With the support of the International Atomic Energy Agency (IAEA), the calibration facility has participated in various activities and has become a member of the Joint Network of Secondary Standard Dosimetry Laboratory (SSDL) of the International Atomic Energy Agency / the World Health Organization (IAEA/WHO).

Recently, the gamma irradiation system of INST has been upgraded using a gamma multi-source irradiation system with ^{137}Cs and ^{60}Co sources to enhance the accuracy of reference air kerma and become the national standard of Vietnam in radiation metrology.

The gamma reference field has established at INST since 2020 using an experimental method with a calibrated ionization chamber. Characteristics of the gamma reference field, such as gamma fluence Φ , mean energy E_ϕ , kerma weighted mean energies E_K , air kerma K_{air} , contribution of the scattered component, and operational dose quantities such as ambient dose equivalent and personal dose equivalent are derived from air kerma through

corresponding conversion coefficients that need to be determined with high accuracy in accordance with the international standard ISO 4037 [1, 2, 3]. The experimental method used at INST directly determine the air kerma, contribution of the scattered component, and operational dose quantities using the ionization chamber, but the gamma fluence Φ , mean energy E_ϕ , kerma weighted mean energies, E_K , could not be determined.

In this work, the MCNP6 simulation code [4] was used to simulate the gamma fluence spectra of ^{137}Cs and ^{60}Co sources. The others characteristics of the reference field, including kerma weighted mean energies E_K and field size, were also determined.

II. MATERIAL AND METHOD

A. Gamma calibration facility

The gamma irradiation room constructed of ordinary concrete has inner dimensions of

875cm x 435cm x 330 cm. The distances from the source to the surrounding walls are 112 cm, 220 cm, 220 cm, and 763 cm, respectively. The distances from the source center to the floor and ceiling are 120 cm and 210 cm, respectively. The lead doors were replaced with concrete walls. This is not expected to affect the simulation results of the reference field characteristics inside the room. The irradiation system includes three ^{137}Cs sources and three ^{60}Co sources. In this work, only the 1.1 Ci ^{137}Cs and the 5 Ci ^{60}Co sources were used in the simulation. The gamma sources were installed in a container on the floor of the irradiation room. When the calibration is performed, the gamma source is pumped up to the exposure position by the a pneumatic system.

The beam collimator has a truncated cone shape conforming to the ISO 4037-1:2019 and is made of lead and tungsten. All the material compositions were taken from Ref. [5] and are presented in Table I.

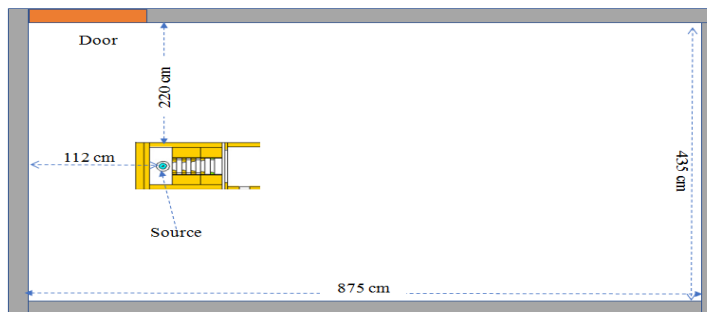


Fig. 1. Top view of the gamma irradiation room

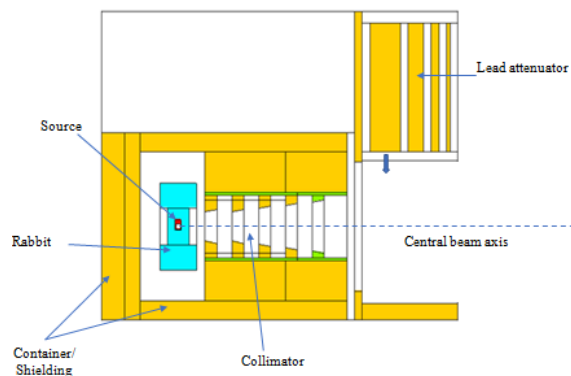


Fig.2: The multi-source irradiation system

Table I. Material density (g/cm³) and weight fraction (%)

Material and density	Air	Aluminum	Lead	Tungsten	Steel	Concrete
H (Z = 1)	0.00121	2.699	11.34	19.25	8.0	2.3
C (Z = 6)	0.012				0.030	0.248
N (Z = 7)	75.527					
O (Z = 8)	23.178					47.493
Na (Z = 11)						1.521
Mg (Z = 12)						0.127
Al (Z = 13)		100.0				1.995
Si (Z = 14)					1.0	30.463
P (Z = 15)					0.045	
S (Z = 16)					0.03	
Ar (Z = 18)	1.283					
K (Z = 18)						1.005
Ca (Z = 20)						4.295
Cr (Z = 24)					17.0	
Mn (Z = 25)					2.0	
Fe (Z = 26)					65.395	0.644
Ni (Z = 28)					12.0	
Mo (Z = 42)					2.50	
W (Z = 74)				100.0		
Pb (Z = 82)			100.0			

B. Main characteristic quantities of the gamma reference field

Characteristics of the gamma reference field, such as total fluence, Φ , air kerma, K_{air} , and kerma weighted mean energy, E_K , can be calculated from the gamma fluence based on equations (1 - 3).

$$\Phi = \int_0^{E_{max}} \Phi_E(E) \cdot dE \quad (1)$$

$$K_{air} = \int_0^{E_{max}} \Phi_E \cdot k(E) \cdot dE \quad (2)$$

$$E_K = \frac{\int_0^{E_{max}} \Phi_E \cdot k(E) \cdot E \cdot dE}{\int_0^{E_{max}} \Phi_E \cdot k(E) \cdot dE} \quad (3)$$

Where, $\Phi_E(E)$ is the photon fluence of energy between E and E+dE. ; $k(E)$ is photon fluence-to-air kerma coefficient [6]

Gamma fluence spectra at distances from 80 to 400 cm inside a sphere of diameters from 2 to 10 cm were simulated using tally F4 in MCNP6.

D. Scattered contribution

Accordingly, ISO 4037-1:2019 defines two components as the air kerma outside the collimated beam and the air kerma inside the collimated beam instead of the scattered beam and direct beam in the previous definition. The radiation outside the collimated beam can be due to scattered radiation by the environment and due to leakage radiation of the source safety enclosure and collimator scatter. The radiation inside the collimated beam includes that scattered from the source capsule, the source shielding, and the collimator. The contribution of the scattered component can be

determined by the deviation from the inverse-square law of the source distance. Thus, the air kerma value at each distance, after correction for scattering by air, will be normalized to a distance of 100 cm as shown in Eq. 4, where $K_{nor}(d)$ is the normalized air kerma at the distance d after correcting for scattering by air. The linear attenuation coefficient of air was obtained from the US National Institute of Standards and Technology database [7].

$$K_{nor}(d) = \frac{K_{air}(d).d^2}{K_{air}(100).100^2} \quad (4)$$

Where, $K_{air}(d)$ is air kerma at the distance d (cm).

E. Reference field size

The reference field size is the maximum distance at which the air kerma value deviates by 5% from the value at the center of the radiation field. At each distance, the distribution of kerma on a plane perpendicular to the central axis was simulated using the FMESH tally and FM card. Each cell in the FMESH tally has a size of 4 cm along the X-axis and 2 cm along the Y- and Z-axes. This tally also allows the determination of air kerma according to equation (2). The intersection of these perpendicular planes with the central beam axis is considered the center of the radiation field. Horizontal points relative to the field center are on the Y-axis, and vertical points relative to the field center are on the Z-axis.

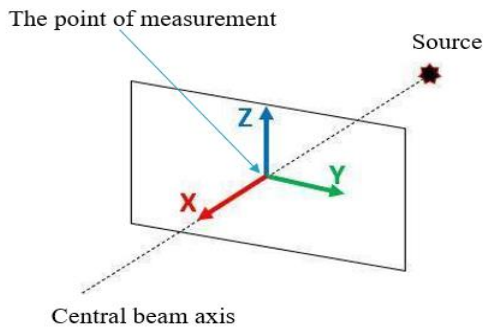


Fig. 3. The plane of measurement to determine the field size

III. RESULTS AND DISCUSSION

A. Main characteristic quantities of the gamma reference field

1. Gamma fluence spectra

The simulated gamma fluence rate spectra of the ^{137}Cs and ^{60}Co sources are shown in Fig.4. The gamma fluence is adjusted for the source's activity on January 1, 2023.

The simulated gamma fluence rate spectra of ^{137}Cs shows an energy peak at 662 keV, and the Compton scattered photon. The 662 keV energy peak is gamma radiation emitted from the source and then reaches the detector without any collisions. Compton region is caused by scattered photons. The fluence of the 662 keV peak is two orders of magnitude larger than the Compton region. The gamma fluence spectrum of the ^{60}Co source also shows two gamma peaks at 1173 keV and 1332 keV and a Compton region due to gamma scattering.

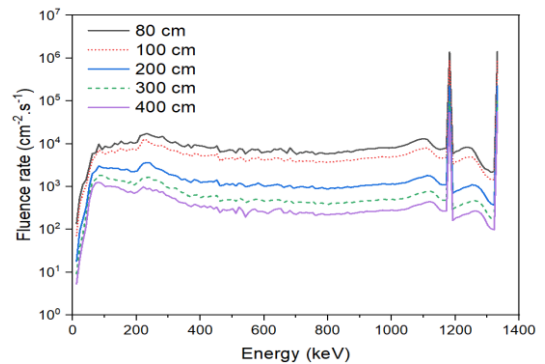
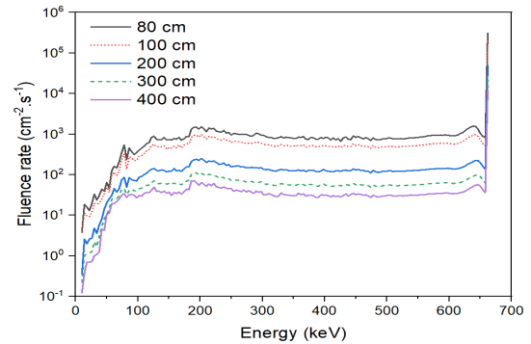


Fig. 4. Gamma fluence spectra at various distances: ^{137}Cs source (left) ; ^{60}Co source (right)

2. Air kerma, Fluence and kerma-weighted mean energy

Tables II and III present the simulated values of air kerma, total fluence, and kerma-weighted mean energy at distances from 80 to 400 cm for both ^{137}Cs and ^{60}Co sources. To be able to compare with the experimental air kerma, the simulated values are adjusted for source activity at the same time.

The last column of table II and III show the air kerma percentage of direct gamma reaching the detector without collision (662 keV for ^{137}Cs ; 1173 keV and 1332 keV for ^{60}Co) to total air kerma. Because the direct air kerma component only accounts for between 80% and 84% of the total kerma value, the contribution of the scattered component should be taken into account when calculating the conversion coefficient from air kerma to operational dose quantities, such as ambient dose equivalents.

Table II. Air kerma and some characteristic quantities of ^{137}Cs reference field

Distance (cm)	Total air kerma ($\mu\text{Gy/h}$)			Φ ($\text{cm}^{-2}\cdot\text{s}^{-1}$)	E_K (keV)	Direct air kerma / Total air kerma
	Simulation	Experiment	Deviation			
80	4260.2	4096.9	3.99%	4.38E+05	622.9	80.95%
90	3360.1	3246.3	3.51%	3.46E+05	622.9	81.03%
100	2717.7	2607.6	4.22%	2.80E+05	622.9	81.08%
120	1882.2	1815.2	3.69%	1.94E+05	622.9	81.16%
150	1201.1	1158.1	3.71%	1.24E+05	622.7	81.18%
200	672.5	664.3	2.79%	6.96E+04	622.5	81.19%
250	428.9	419.2	2.32%	4.45E+04	622.0	81.10%
300	296.8	290.9	2.02%	3.09E+04	621.6	81.02%
350	217.4	212.5	2.31%	2.27E+04	621.0	80.90%
400	166.0	162.8	1.97%	1.75E+04	620.3	80.75%

Table III. Air kerma and some characteristic quantities of ^{60}Co reference field

Distance (cm)	Total air kerma ($\mu\text{Gy/h}$)			Φ ($\text{cm}^{-2}\cdot\text{s}^{-1}$)	E_K (keV)	Direct air kerma / Total air kerma
	Simulation	Experiment	Deviation			
80	64060	63954	0.16%	3.83E+06	1192	83.42%
90	50461	50138	0.64%	3.02E+06	1192	83.59%
100	40794	40736	0.14%	2.45E+06	1192	83.70%
120	28245	28253	0.03%	1.70E+06	1192	83.82%
150	18022	18088	0.37%	1.10E+06	1191	83.90%
200	10103	10100	0.04%	6.22E+05	1189	83.88%
250	6452	6536	1.29%	4.02E+05	1188	83.77%
300	4471	4521	1.10%	2.81E+05	1186	83.68%
350	3278	3296	0.54%	2.07E+05	1185	83.57%
400	2506	2521	0.61%	1.60E+05	1184	83.41%

The difference between the simulated and experimental kerma values is 4.22% for the ^{137}Cs source and 1.29% for the ^{60}Co source. Because the uncertainty of activity of the sources are not reported in the certificate, the agreement between the experimental and simulation results cannot be evaluated. However, the difference is less than 5%, indicating that the simulated gamma fluence spectra of the radiation standard field using MCNP6 can be used to calculate other characteristic quantities of the standard field.

The kerma-weighted mean energy gradually decreases with increasing the source-detector distance because the contribution of scattered component increases with distance.

However, the origin scatted component due to different component of the calibration room (e.g: air, collimator, wall) requires further detailed simulation.

B. Scattering contribution

The deviation from the inverse-square law of the source-chamber distance of kerma values for both ^{137}Cs and ^{60}Co sources is shown in Fig.5.

The contribution of the scattered photons of both ^{137}Cs and ^{60}Co sources is less than 3.5% with both simulation and experimental methods. These results ensure that the gamma reference fields comply with the scattering criteria of the ISO 4037:2019.

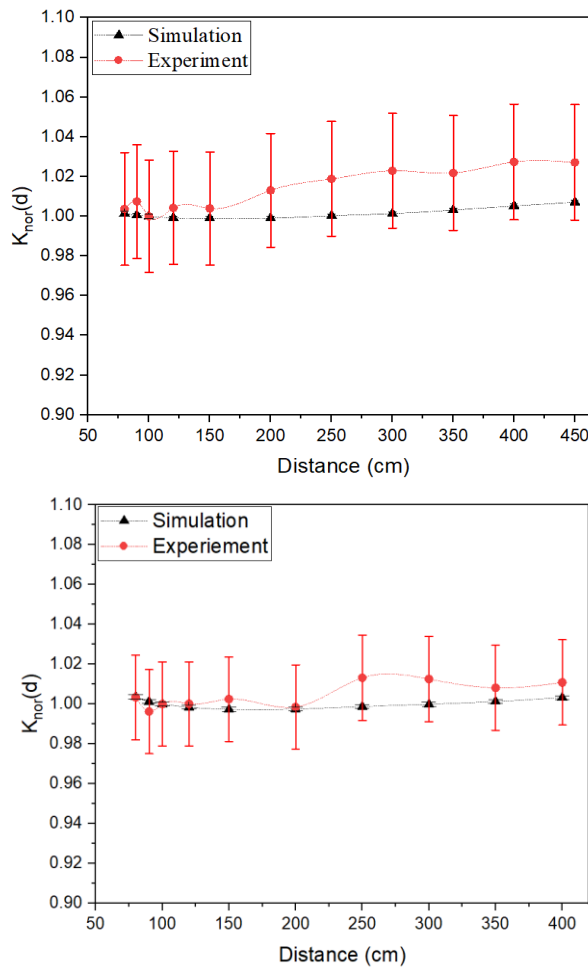


Fig. 5. Deviation from the inverse-square law: ^{137}Cs source (left) ; ^{60}Co source (right)

C. Reference field size

The normalized air kerma distribution at a distance of 100 cm in the horizontal axis (Y-axis) and vertical axis

(Z-axis) is shown in Fig. 6. From this distribution, the radiation field sizes of the ^{137}Cs and ^{60}Co sources were determined as shown in Fig.7.

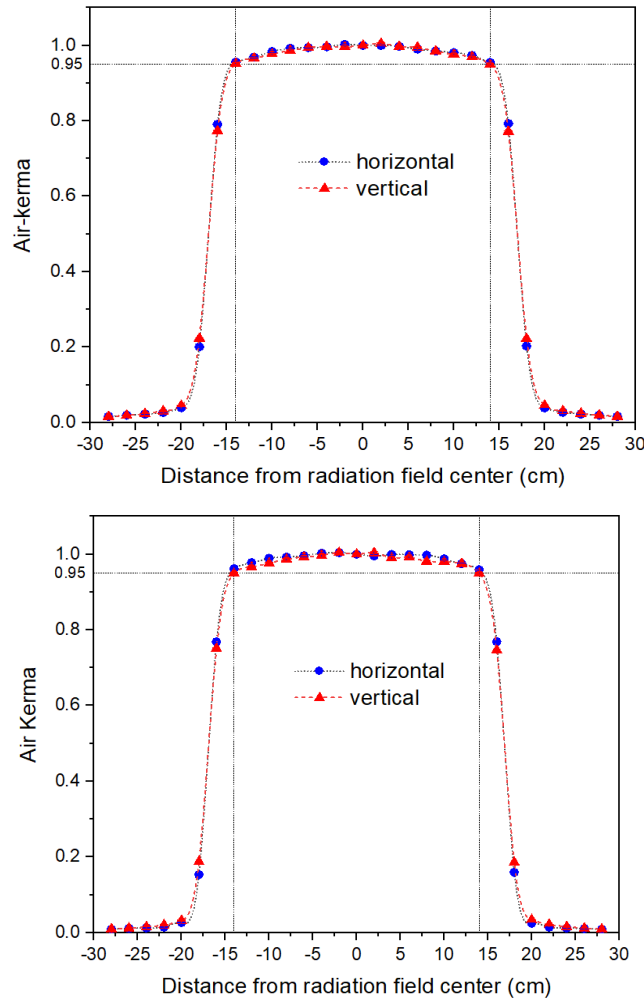


Fig. 6. Kerma distribution at a distance 100 cm from source: ^{137}Cs source (left) ; ^{60}Co source (right)

The normalized air kerma distributions at planes perpendicular to the central axis along the Y and Z axes overlap each other. This can be explained by the symmetrical configuration of the multi-source gamma irradiation system, and the influence of scattered photons from the room is not much different. Furthermore, the kerma distributions of ^{137}Cs and ^{60}Co sources were almost identical.

From the kerma distribution at each distance, the radiation field size was determined to ensure that the uniformity of the radiation field is less than 5% [1]. Because the spatial resolution of the simulated air kerma distribution is from 2 cm to 5 cm and the scattering component ratios are different at each distance, the radius of the radiation field is not entirely linear with distance.

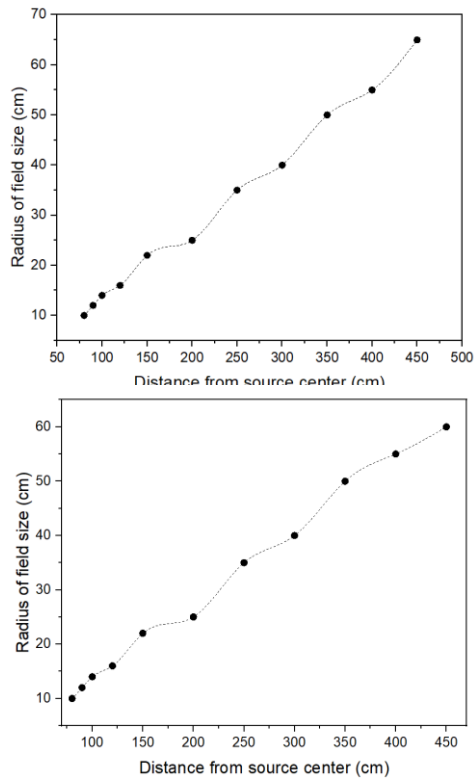


Fig. 7. Reference field size: ^{137}Cs (left side); ^{60}Co (right side)

IV. CONCLUSION

This study has performed simulation of the gamma reference fields at INST using the MCNP6 code. The air kerma difference between experiment and simulation of less than 5% confirms the reliability of the simulation results. The simulation method also provides additional information about the reference field, such as photon fluence, mean energy that the experimental method lacked. Combined with the experimental data, the gamma reference fields complies with the ISO 4037:2019 standard.

ACKNOWLEDGMENTS

This study was funded by the Ministry of Science and Technology under the grant code: ĐTCB.05/23/VKHKTHN.

REFERENCES

- [1]. ISO, Radiological protection - X and gamma reference radiation for calibrating dosimeters and doserate meters and for determining their response as a function of photon energy - Part 1: Radiation characteristics and production methods, ISO 4037, 2019.
- [2]. ISO, Radiological protection - X and gamma reference radiation for calibrating dosimeters and doserate meters and for determining their response as a function of photon energy - Part 2: Dosimetry for radiation protection over the energy ranges from 8 keV to 1,3 MeV and 4 MeV to 9 MeV, ISO 4037, 2019.
- [3]. ISO, Radiological protection - X and gamma reference radiation for calibrating dosimeters and doserate meters and for determining their response as a function of photon energy - Part 3: Calibration of area and personal dosimeters and the measurement of their response as a function of energy and angle of incidence, ISO 4037, 2019.
- [4]. Denise B. Pelowitz, MCNP6 User's Manual (Version 1.0), LA-CP-13-00634, 2013.
- [5]. P.N.N. Laboratory, Compendium of Material Composition Data for Radiation Transport Modeling, PNNL-15870, Rev. 2. (2021).
- [6]. ICRU, Operational Quantities for External Radiation Exposure, ICRU Report 95, 2020.
- [7]. Hubbell J. H., Seltzer, S. M., Tables of X-Ray Mass Attenuation Coefficients and Mass Energy-Absorption Coefficients (version 1.4), National Institute of Standards and Technology, 2004.
- [8]. Harald. Dombrowski, On the conversion coefficient from air kerma to ambient dose equivalent valid for a ^{137}Cs photon field – A critical reviews, Radiation Protection Dosimetry, 2018.